Prolyl isomerase Pin1 regulates axon guidance by stabilizing CRMP2A selectively in distal axons

Martin Balastik[1,2,3,†], **Xiao Zhen Zhou**[1], **Meritxell Alberich-Jorda**[1,2], **Romana Weissova**[2,3], **Jakub Žiak**[2,3], **Maria F. Pazyra-Murphy**[4,5], **Katharina E Cosker**[4,5], **Olga Machonova**[2], **Iryna Kozmikova**[2], **Chun-Hau Chen**[1], **Lucia Pastorino**[1], **John M. Asara**[1], **Adam Cole**[6], **Calum Sutherland**[6], **Rosalind A. Segal**[4,5], and **Kun Ping Lu**[1,7,†]

[1]Department of Medicine Beth Israel Deaconess Medical Center, Harvard Medical School, 330 Brookline Avenue, CLS 0408, Boston, MA 02215, USA

[2]Institute of Molecular Genetics, Víde ská 1083, 142 20 Prague 4, Czech Republic

[3]Institute of Physiology, Víde ská 1083, 142 20 Prague 4, Czech Republic

[4]Department of Pediatric Oncology and Cancer Biology Dana-Farber Cancer Institute, Boston, MA 02215, USA

[5]Department of Neurobiology Harvard Medical School, Boston, MA 02115, USA

[6]Biomedical Research Institute University of Dundee, Ninewells Hospital Dundee, Scotland, DD1 9SY, UK

[7]Institute for Translational Medicine Fujian Medical University Fuzhou, China 350108

SUMMARY

Axon guidance relies on precise translation of the gradients of the extracellular signals into local changes of cytoskeletal dynamics, but the molecular mechanisms regulating dose-dependent responses of growth cones are still poorly understood. Here we show that during embryonic development in growing axons low level of Semaphorin3A stimulation is buffered by the prolyl isomerase Pin1. We demonstrate, that Pin1 stabilizes CDK5-phosphorylated CRMP2A, the major isoform of CRMP2 in distal axons. Consequently, Pin1 knockdown or knockout reduces CRMP2A level specifically in distal axons and inhibits axon growth, which can be fully rescued by Pin1 or CRMP2A expression. Moreover, Pin1 knockdown or knockout increases sensitivity to Sema3A-induced growth cone collapse in vitro and in vivo leading to developmental abnormalities in axon guidance. These results identify an important isoform-specific function and regulation of CRMP2A in controlling axon growth, and uncover Pin1-catalyzed prolyl isomerization as a regulatory mechanism in axon guidance.

[†]All correspondence should be addressed to Kun Ping Lu, Tel 617-735-2016, Fax 617-735-2050, klu@bidmc.harvard.edu; or Martin Balastik, martin.balastik@fgu.cas.cz.

INTRODUCTION

During development of the nervous system, axonal growth is tightly regulated by an array of extracellular secreted and membrane-bound cues that interact with their receptors at the active growth cones. These interactions trigger signaling cascades that alter microtubule dynamics resulting in axonal growth, turn, stop, or retraction. While many extracellular cues and their receptors have been discovered within the last two decades (Culotti and Kolodkin, 1996; Tessier-Lavigne and Goodman, 1996), little is known about how the signaling cascades they trigger are integrated into a single unified response.

A key player in translating upstream signaling cascades into axon growth and collapse is collapsin response mediator protein 2 (CRMP2), a tubulin heterodimer-binding protein that promotes microtubule assembly (Fukata et al., 2002) and axon growth (Fukata et al., 2002; Inagaki et al., 2001; Yoshimura et al., 2005). Importantly, upon its CDK5/GSK-3β- or Rho kinase-mediated phosphorylation the affinity of CRMP2 to tubulin is dramatically reduced which shifts the dynamic equilibrium of microtubules towards their disassembly (Arimura et al., 2000; Arimura et al., 2005; Uchida et al., 2005; Yoshimura et al., 2005). Consequently, stimulation of growing axons with Sema3A, which activates CDK5 (Sasaki et al., 2002) leading to CRMP2 phosphorylation (Cole et al., 2004; Uchida et al., 2005; Yoshimura et al., 2005), promotes growth cone collapse (Cole et al., 2004; Uchida et al., 2005; Yoshimura et al., 2005).

An alternative splicing of *Crmp2* gene has been recently shown to generate two isoforms that differ in their N-terminus: CRMP2B and an ~ 100 amino acids longer CRMP2A (Quinn et al., 2003; Yuasa-Kawada et al., 2003). Little is known about CRMP2A that has been reported to localize in axons rather than dendrites (Quinn et al., 2003; Yuasa-Kawada et al., 2003) and was speculated to be regulated by conformational changes (Schmidt and Strittmatter, 2007).

Conformational changes may represent an important regulatory mechanism in axon guidance as they enable a rapid change of protein activity, which is vital to ensure the correct response of a growing axon to its changing environment. We have previously shown that pSer/Thr-Pro motifs in certain proteins can exist in two distinct *cis* and *trans* conformations and identified prolyl isomerase Pin1 that specifically accelerates their conversion to regulate phosphorylation signaling (Yaffe et al., 1997). Furthermore, phosphorylation dramatically slows down the already slow rate of isomerization of Ser/Thr-Pro bonds, and renders the phosphopeptide bond resistant to the catalytic action of all other PPIases, with exception of Pin1 (Yaffe et al., 1997). Significantly, Pin1 is tightly regulated on multiple levels and its deregulation has an important role in a growing number of pathological conditions e.g Alzheimer's disease, where it plays a pivotal role in protecting against age-dependent neurodegeneration (Balastik et al., 2007; Liou et al., 2003; Nakamura et al., 2012; Pastorino et al., 2006). However, little is known about the function of Pin1 in healthy neurons and during development of the nervous system.

Here, using a proteomic approach we identify CRMP2A as a major Pin1 target in postnatal neurons. Our results not only identify an important isoform-specific function for CRMP2A

in regulating axon growth through Pin1-driven conformational stabilization of phosphorylated CRMP2A selectively in distal axons, but also uncover a mechanism regulating axon guidance in Sema3A gradients by Pin1 both *in vitro* and *in vivo*.

RESULTS

Proteomic approach identifies CRMP2A as a major Pin1 substrate in neurons

To determine the role of Pin1 in healthy neurons, we used a GST-Pin1 affinity purification procedure under high-salt and -detergent conditions to identify Pin1 substrates in postnatal brains. Following SDS-PAGE and tandem mass spectrometry (LC-MS/MS), one prominent and reproducibly pulled down protein was identified as collapsin response mediator protein 2 (CRMP2) (Fig. 1A, S1). Two splice forms of CRMP2 have been identified: a shorter CRMP2B (~62 kDa) (Fukata et al., 2002; Inagaki et al., 2001) and a longer CRMP2A (~73 kDa) (Yuasa-Kawada et al., 2003). The molecular weight of the Pin1-bound CRMP2 was ~73 kDa (Fig. 1A), which is significant given that the shorter CRMP2B is ~20 times more abundant than CRMP2A in brain lysates (Yuasa-Kawada et al., 2003), suggesting that Pin1 might preferentially bind to CRMP2A.

To test this possibility, we overexpressed FLAG-CRMP2A and -CRMP2B in SH-SY5Y neuroblastoma cells and analyzed their binding to Pin1. Since Pin1 binds its substrates only upon their phosphorylation (Lu et al., 2007; Lu and Zhou, 2007), we arrested the transfected SH-SY5Y cells in mitosis with nocodazole, which increases concentration of mitotic proline-directed kinases (Lu et al., 1999a). The GST-Pin1 pulldown assay confirmed Pin1 binding to CRMP2A (but not to CRMP2B) only in the presence of nocodazole (Fig. 1B, fl-CRMP2B, fl-CRMP2A), suggesting that phosphorylation of CRMP2A is necessary for the binding. To detect interaction between endogenous Pin1 and CRMP2A in vivo, we immunoprecipitated Pin1 from brain lysates of Pin1 wild-type (WT) and Pin1 knockout (KO) mouse embryos at E17.5. CRMP2A co-immunoprecipitated with Pin1 from WT brain lysates, but not Pin1 KO controls (Fig. 1C). These results indicate that Pin1 forms stable complexes selectively with CRMP2A in vitro and in vivo.

By analyzing 5' sequence of CRMP2A, we found that it contains a single putative Pin1 binding site around Ser27, which is highly evolutionarily conserved, but not present in other CRMP family members (Fig. 1D). More importantly, analysis of the sequence with scansite (scansite.mit.edu) predicted Ser27 to be a likely CDK5 phosphorylation site. To determine whether Ser27 is indeed phosphorylated in CRMP2A, we overexpressed FLAG-CRMP2A in HEK-293T cells together with CDK5/p25 kinase and immunoprecipitated FLAG-CRMP2A with anti-FLAG M2 monoclonal antibody beads. After elution from FLAG-beads with FLAG peptide, the purified CRMP2A was subject to GST-Pin1 pulldown and LC-MS/MS analysis. C-terminal Ser623 in the Pin1 bound CRMP2A fraction was phosphorylated (Fig. 1E, G), as shown before for analogous Ser522 phosphorylation in CRMP2B (Gu et al., 2000). Importantly, Ser27 in CRMP2A was indeed phosphorylated in the Pin1-bound fraction (Fig. 1E, F), suggesting that Ser27 phosphorylation might be required for Pin1 binding. To confirm this possibility, we generated S27A mutant of CRMP2A and tested its binding to Pin1 in SH-SY5Y cells. S27A mutation significantly reduced CRMP2A binding to Pin1 (Fig.1B, I –S27A), demonstrating its importance for the Pin1-CRMP2A interaction.

In order to test whether the C-terminal CDK5 phosphorylation site also participates on interaction with Pin1, we generated single S623A, and double S27,623A mutants and compared their binding to Pin1 in SH-SY5Y, co-transfected with CDK5/p25 (Fig. 1H, I). Similar to S27A, single S623A mutation significantly reduced Pin1 binding and S27,623A double mutation totally abolished Pin1 binding to CRMP2A. Notably, CRMP2B is known to be phosphorylated on S522, a site equivalent to S623 of CRMP2A (Gu et al., 2000; Uchida et al., 2005). Thus, our findings that Pin1 binds to CRMP2A, but not CRMP2B (Fig. 1B), indicate that the critical role in mediating CRMP2A interaction with Pin1 is played by Ser27 phosphorylation.

Pin1 stabilizes CRMP2A phosphorylated by CDK5

Since Pin1 regulates protein stability of many of its substrates (Lu et al., 2007; Lu and Zhou, 2007), we asked whether CDK5 phosphorylation and Pin1 binding affects protein stability of CRMP2A. We generated stable Pin1 knockdown (KD) HEK-293T cells using shPin1 or control non-silencing shRNA (NSC) lentiviruses (Fig. 2A) and then introduced FLAG-tagged CRMP2A together with CDK5/p25 into these cells. Cells were treated with cycloheximide to inhibit de novo CRMP2A synthesis, followed by immunoblotting with the anti-FLAG antibody at various times. Under this cycloheximide chase FLAG-CRMP2A was readily detectable at ~6 hr in NSC control cells (Fig. 2B, C), but its degradation was greatly accelerated in Pin1 KD cells (sh-Pin1, Fig. 2B, C). To see whether CDK5 phosphorylation triggers degradation of CRMP2A by proteasome, we analyzed protein stability of FLAGCRMP2A transfected into HEK-293T cells with or without CDK5/p25 in the absence or presence of proteasome inhibitor MG132. Cotransfection with CDK5 potently reduced CRMP2A levels, which were largely abrogated by MG132 (Fig. 2D, E). Moreover, S27A mutation significantly stabilized CRMP2A after co-transfection with CDK5/p25, and MG132 treatment did not lead to further stabilization (Fig. 2D, E). These data indicate that phosphorylation of Ser27 by CDK5 promotes proteasomal degradation of CRMP2A, but that Pin1 renders phosphorylated CRMP2A stable.

Next, we tested whether changes in levels of CRMP2A or Pin1 affect also CRMP2B levels due to know CRMP2 tetramerization. We generated a shRNA lentiviral vector specifically targeting CRMP2A, but not CRMP2B (Fig. 2F) and examined changes of endogenous CRMP2A and CRMP2B in SH-SY5Y cells after KD of CRMP2A or Pin1. As expected, Sh-CRMP2A lentivirus effectively knocked down endogenous CRMP2A, but did not significantly affect CRMP2B levels (Fig. 2G, H). Moreover, Pin1 KD also significantly reduced CRMP2A without affecting CRMP2B (Fig. 2G, H). Next, to examine whether Pin1 also affects CRMP2A level in primary neurons, we cultured E15.5 Pin1 WT primary cortical neurons, infected them with either shPin1 or non-silencing lentiviruses and compared their CRMP2A and CRMP2B levels to those in Pin1 KO primary neurons. Pin1 KD or KO significantly reduced total CRMP2A levels by ~40% (Fig. 2J, K). Western blotting of primary neuron lysates revealed the presence of multiple CRMP2A bands, suggestive of phosphorylated CRMP2A. Indeed, treating the lysates with λ phosphatase resulted in complete loss of the upper bands (Fig. 2I), confirming that the mobility shift is due to CRMP2A phosphorylation. Significantly, Pin1 KD or KO reduced phosphorylated CRMP2A levels even more (~65% reduction) than total CRMP2A levels (Fig. 2J,L),

consistent with the fact that Pin1 acts on its substrates after phosphorylation (Lu et al., 1999b). Neither KO nor KD of Pin1 affected CRMP2B levels (Fig. 2G). Finally, using primary cortical neurons at 6 DIV, we detected endogenous phosphorylated CRMP2A levels rapidly decreasing in a cycloheximide chase in Pin1 KO neurons, but not in Pin1 WT neurons (Fig. 2M, O). Neither, we detected a significant change in CRMP2B levels (Fig. 2M, N). Together these results indicate that Pin1 specifically binds to CRMP2A phosphorylated by CDK5 and prevents its proteasomal degradation.

CRMP2A is the dominant isoform in the distal axons, where it is stabilized by Pin1

Next, we analyzed the distribution of CRMP2A in the primary neuronal cultures. CRMP2A was detected in neuronal cell bodies and to a lesser extent in dendrites, as identified by co-staining with the neuron marker βIII tubulin (Fig. S2A) and the dendritic marker MAP2 (Fig. S2C). Notably, particularly high levels of CRMP2A were found in WT distal axons close to the growth cones, as detected by the axon marker tau (Fig. S2B), but in Pin1 KO neurites CRMP2A was significantly reduced (Fig. 3A, B). Moreover, similar results were also obtained by knocking down Pin1 in Pin1 WT or Pin1+/− neurons (Fig. 3J, K, S2D, E). Quantification of the CRMP2A signals in the axon shaft revealed a 64% reduction of CRMP2A levels ($p < 0.0001$) upon Pin1 KD (Fig. 3N), while no significant difference was detected in the neuron cell body ($p= 0.523$) (Fig. 3M). Thus, Pin1 KO or KD reduces CRMP2A levels specifically in the axons, with little effect on the perikaryal levels.

Unexpectedly, total CRMP2 signals, as detected by antibodies recognizing both CRMP2A and CRMP2B, were also significantly reduced in distal axons after Pin1 KD (44% reduction, $p=0.0005$) (Fig. 3J, K, M, N, S2). These results are rather surprising given the previous findings that CRMP2B is ~20 times more abundant than CRMP2A in total brain lysates(Yuasa-Kawada et al., 2003). They suggest that CRMP2A could be the dominant isoform of the CRMP2 pool in the vicinity of the growth cone.

In order to gain a better insight into the distribution of the two CRMP2 isoforms in neurons, we used compartmented cultures of dorsal root ganglia (DRG) neurons with Campenot chambers that allow separation of cell bodies and proximal axons (CB + PA) from distal axons (DA) in growing neurons (Fig. 3G) (Pazyra-Murphy and Segal, 2008). First we analyzed the distribution of Pin1 and CRMP2A in DRG neurons isolated from Pin1 WT and Pin1 KO mouse E12.5 embryos by double-immunostaining. A weak CRMP2A signal was detected in the CB + PA compartments of both Pin1 WT and KO DRG neurons (Fig. 3C, E), but a strong expression of CRMP2A was found in the DA of Pin1 WT DRG, which co-localized with Pin1 (Fig 3D). In contrast, in Pin1 KO DRG there was only a weak CRMP2A signal in the DA compartment (Fig. 3F). In order to obtain enough protein lysates to be able to quantify CRMP2A and CRMP2B levels in DA and CB+PA compartments by western blotting, we prepared DRG compartmented cultures from WT rat E14.5 embryos. Analysis of protein lysates isolated from the two compartments revealed that while CRMP2A levels were not significantly different between DA and CB+PA ($p<0.38$) (Fig. 3H, I), the levels of CRMP2B in DA were significantly lower ($p<8.5E-06$) in CB + PA compartments, more than 11 times (Fig. 3H, I), suggesting an increased role of CRMP2A in distal axons (Fig. 3G). In order to estimate the relative content of CRMP2A and CRMP2B directly in the

vicinity of growth cones, we used CRMP2A-specific shRNA lentiviruses to specifically silence CRMP2A in primary cortical neurons and calculated the relative contribution of CRMP2A and CRMP2B in the axon shaft and neuron cell bodies indirectly from changes of CRMP2A and total CRMP2 signals. CRMP2A KD reduced CRMP2A signals both in the cell body and the neurite by 89% and 82%, respectively (p <0.0001), confirming the specificity of both the shCRMP2A construct and the CRMP2A antibodies (Fig. 3J, L, O, P, S2). Interestingly, upon CRMP2A KD, total CRMP2 levels decreased only 33% in neuronal cell bodies (p<0.0001) (Fig. 3J, L,O), but dropped more than 60% in axon shafts (p<0.0001) (Fig. 3J, L, P, S2D, F). Based on these data, we calculated that although CRMP2A represented only a minority (~40%) of the total CRMP2 level in neuronal cell bodies (Fig. 3Q) of primary cortical neurons, it accounted for 70% of the total CRMP2 pool in the axon shafts (Fig. 3Q). To further confirm these results, we performed similar calculations upon Pin1 KD (Fig. 3J, K) because in our previous experiments Pin1 KD specifically reduced CRMP2A, but not CRMP2B levels (Fig. 2G, J, M). Similar results were again obtained, with CRMP2A contributing to 69% of the total CRMP2 pool in the axon shafts. Thus, CRMP2A is the dominant isoform in the growth cone vicinity, where it is stabilized by Pin1.

Pin1 acts on CRMP2A to promote axon growth in vitro

Given Pin1 stabilizes CRMP2A in distal axons, we analyzed whether modulating Pin1 or CRMP2A levels would yield a significant effect on axon growth. We used lentiviral vectors to silence or overexpress Pin1 or CRMP2A in E15.5 primary cortical neurons isolated from Pin1 WT embryos and compared their axon lengths after 3 days in cultures. While Pin1 overexpression did not have a significant effect on axon length (Fig. 4A, B, F), KD of either Pin1 or CRMP2A led to a significant (~40%) reduction of axon length compared to neurons infected with a non-silencing lentiviral vector (Fig. 4C–F). To confirm these results, we performed similar experiments using Pin1 KO primary cortical neurons. While, as expected, Pin1 KD had no effect (Fig. 4J, K, L), CRMP2A KD resulted in a small, although not statistically significant decrease in axon length (Fig. 4I, J, K, L), likely due to the fact that CRMP2A in Pin1-deficient axons is already very low (Fig. 2E, I). Importantly, re-expression of Pin1 in Pin1 KO neurons fully rescued their axon length to the WT levels (Fig. 4G, H, L).

In order to test whether it is the isomerase activity of Pin1 that plays a role in axon growth, we analyzed the effect of juglone, a specific inhibitor of Pin1 isomerase activity (Hennig et al., 1998). Indeed, treatment of WT primary cortical neurons at 1DIV for 3 days resulted in a significant (p < 2e-06) reduction of axon growth and CRMP2A levels in neurites (Fig. S3), similar to the effect observed with Pin1 KO or KD (Fig. 4 A, D, G, F).

Next, we tested whether overexpression of CRMP2A can rescue the reduced axon growth in Pin1 KO neurons. E15.5 Pin1 WT and KO primary cortical neurons were transfected with FLAG-CRMP2A or a vector control together with GFP to mark the transfected cells, fixed after 6 days, stained for FLAG-CRMP2A, traced and quantified for axonal length. Similar to the endogenous CRMP2A (Fig. 3, S2), FLAG-CRMP2A was localized in Pin1 WT and KO neurons primarily in distal axons and cell bodies (Fig. S3E, G). Pin1 WT cortical neurons transfected with CRMP2A did not show any significant increase in their axon length, as

shown before (Yuasa-Kawada et al., 2003) (Fig. 4M, O). Similar to the above experiments (Fig. 4G), Pin1 KO neurons had significantly shorter axons, but their axon growth was fully rescued by CRMP2A overexpression (Fig. 4N, P, S3) even beyond the WT length, which is likely due to overcompensation. These results together indicate that Pin1 stabilizes CRMP2A in distal axons to promote axon growth.

Pin1 buffers Semaphorin3A-induced growth cone collapse in vitro

Activation of CDK5 and subsequent phosphorylation and inactivation of CRMP2 has been shown to be a necessary step in Semaphorin 3A (Sema3A)-induced growth cone collapse (Cole et al., 2004; Uchida et al., 2005). In a broader context, Pin1-dependent regulation of CRMP2A upon CDK5 phosphorylation may therefore represent a regulatory mechanism in Sema3A signaling and axon guidance. To examine this possibility, we first analyzed Pin1 distribution in the active growth cones of primary DRG neurons after stimulation with Sema3A. Interestingly, Sema3A stimulation led to a rapid increase of Pin1 concentration in the vicinity of growth cones (Fig. 5A, C, D), which may reflect Pin1 binding to CRMP2A upon its Sema3A-induced phosphorylation, because Pin1 subcellular localization is driven by its binding to the substrate (Lu et al., 2002). Indeed, CRMP2A strongly co-localized with Pin1 in Sema3A stimulated DRG axons (Fig. 5A) and axons containing high levels of Pin1 also showed strong CRMP2A staining (Fig. 5A). In contrast, lower levels of CRMP2A were detected in the Pin1 KO DRG axons upon Sema3A stimulation (Fig. 5B) suggesting that Pin1 could be stabilizing CRMP2A in the growth cone vicinity.

Next, we examined sensitivity of Pin1 KO DRG neurons to Sema3A stimulation. Pin1 WT and KO DRGs were treated at 1DIV with different concentrations of Sema3A, fixed, immunostained for Pin1, β-actin (to label active growth cones) and β-tubulin (to label axons) and number of collapsed axons was counted. Significantly, growth cone collapse was detected in Pin1 KO DRG neurons treated with 0.01 nM Sema3A (Fig. 5F–H, J), whereas in Pin1 WT DRGs after treatment with Sema3A concentrations more than an order of magnitude higher (Fig. 5C–E, J). Moreover, Pin1 levels in the growth cones significantly increased ($p < 4e\text{-}06$) in Pin1 WT DRG neurons upon stimulation with 0.05 nM Sema3A, which did not induce collapse of Pin1 WT neurons, but which was already collapsing Pin1 KO neurons (Fig. 5C, D, I). Furthermore, Pin1 levels significantly ($p < 0.0374$) dropped in Pin1 WT DRGs stimulated with high Sema3A concentrations inducing collapse of most of the growth cones (Fig. 5E, J). These results indicate that Pin1 level in the growth cone vicinity changes during Sema3A stimulation and regulates sensitivity of the growth cones to Sema3A induced collapse.

To test whether the role of Pin1 in growth cone collapse is specific for Sema3A signaling, growth cone collapse was analyzed in Pin1 WT and KO DRGs upon treatment with lysophosphatidic acid (LPA), which has been shown to induce collapse through activation of Rho-kinase and subsequent phosphorylation of CRMP2 at Thr555 (Arimura et al., 2000). Using the same method of analysis as in the previous Sema3A experiment, treatment with 0.1, 1, 10 and 100 μM LPA produced no significant difference in the number of collapsed growth cones between Pin1 WT and KO DRGs (Fig. 5L, S4) and no significant change of Pin1 levels in the growth cones was measured (Fig. 5K, S4). These results indicate that Pin1

is not involved in LPA induced growth cone collapse and further supports that the effect of Pin1 on Sema3A signaling is specific.

Finally, since the effects of the guidance cues depend *in vivo* on their gradient rather than a particular concentration, we tested whether the increased sensitivity of Pin1 KO neurons to Sema3A collapse can be detected also by its gradient application. Mouse E12.5 DRG explants were co-cultured in collagen/matrigel 3D cultures with SH-SY5Y cells expressing Sema3A for 44 hours, fixed, immunostained for NF-M to trace DRG axons, and the average distance of the collapsed axons from the source of the Sema3A gradient was measured. Indeed, while no collapse was detected in Pin1 WT or KO DRG explants cocultured with vector transfected SH-SY5Y cells (Fig. 5M, O), a significant increase (2.1×, p< 2.2e-05) of the average distance of the collapsed neurons from the gradient source was detected in Pin1 KO DRG explants, as compared to Pin WT neurons (Fig. 5N, P, Q). Thus, our data demonstrate in multiple systems that Pin1 specifically buffers low levels of Sema3A stimulation likely via stabilizing CRMP2A in the vicinity of the active growth cones.

Pin1 regulates Sema3A driven axon guidance in embryonic development in vivo

To examine whether Pin1 KO mice display any developmental abnormalities in axon guidance that might be opposite to those in Sema3A- or Nrp-1 KO mice in the peripheral nervous system (Behar et al., 1996; Gu et al., 2003), we performed whole-mount neurofilament immunostaining of Pin1 WT and KO embryos at E12.5. In contrast to Pin1 WT controls, the cranial nerves in Pin1 KO embryos displayed stunted neurite processes and a profound lack of arborization in the axons of the ophthalmic branch of the trigeminal nerve (three out of four Pin1 KO embryos, one out of five Pin1 WT) (Fig. 6A–D). Similarly, Pin1 KO spinal nerves in the cervical region also exhibited stunted and less branched projections (two out of four Pin1 KO embryos and none out of four Pin1 WT) (Fig. 6E–H). Next, to characterize the role of Pin1 in development of the central nervous system, we analyzed entorhino-hippocampal projections (Gu et al., 2003; Pozas et al., 2001) by staining horizontal sections of E15.5 embryonic brains with neurofilament antibodies as a marker. While the entorhinal perforant pathway projections in Pin1 heterozygous embryos at E15.5 had already reached stratum lacunosum-moleculare of the developing hippocampus proper, growth of the Pin1 KO entorhinal projections was significantly slower, reaching the border of subiculum (Fig. 6I–M, three out of three Pin1 KO embryos, none out of three Pin1+/−), which is consistent with the reduced axon growth (Fig. 4) and increased sensitivity to Sema3A (Fig. 5) of Pin1 KO neurons. In addition, WT entorhinal projections showed high levels of CRMP2A, but lower CRMP2A levels were found in Pin1 KO axons (Fig. 6K, L) again corroborating the view of Pin1 as a regulator of axon growth through stabilization of CRMP2A.

Many of the pathfinding errors from the early development of Sema3A KO mice are corrected or eliminated later in development (White and Behar, 2000). To examine whether the defects in Pin1 KO embryos are also later corrected, we analyzed the perforant pathway of the entorhino-hippocampal projection in newborn (P0) and adult (P56) Pin1 WT and KO mice. Indeed, at both postnatal stages the enthorino-hippocampal projections of Pin1 KO were detected in their proper destination: stratum lacunosum-moleculare (Fig. 6N, O, three

Pin1 KO mouse tested), indicating that they are corrected similar to Sema3A KO mice (White and Behar, 2000).

Apart from the Sema3A regulated perforant pathway, entorhinal fibers send their projections via alveus (alvear pathway) (Deller et al., 1996). While little is known about guidance cues regulating development of the alvear pathway, Sema3A plays likely a less important role, since Sema3A KO mice seem to have no defects in alvear pathway, even though aberrant projections were found in the perforant pathway (Pozas et al., 2001). Similarly, neurofilament immunostaining revealed that unlike the perforant pathway, development of the alvear pathway is not affected in the Pin1 KO mice (Fig. S5, three out or three Pin1 KO E15.5 embryos), indicating that the axon growth defects in Pin1 KO mice are not general, but rather restricted to some Sema3A guided projections.

Sema3A deficiency has been shown before to interfere with segregation and fasciculation of somatosensory (S1) and primary motor (M1) cortex neuron projections in corpus callosum (Zhou et al., 2013). In order to characterize the growth and fasciculation of S1 axons in adult Pin1-KO mice, we analyzed DiI labeled S1 axons in corpus callosum. We found that at corpus callosum midline Pin1-KO S1 axons were fasciculated, with fluorescence intensity distribution along the D-V axis similar in Pin1-WT and Pin1-KO mice (~ 120 μm) (Fig. S5), i.e. comparable to the published WT values (Zhou et al., 2013) and significantly more focused than projections in Sema3A-KO or Nrp1-KO mice (~ 300μm) (Zhou et al., 2013). This data are consistent with the hypothesis that Pin1 deficiency potentiates Sema3A signaling, since the phenotype of Pin1-KO S1 projections is opposite to the defasciculated S1 neuron growth in Sema3A-KO mice.

Finally, we tested genetic interaction between Pin1 and Sema3A *in vivo* in developing zebrafish embryos. It has been previously shown that Sema3A controls growth of motor neurons in zebrafish and that reduced Sema3A signaling, through morpholino KD of Sema3A or Neuropilin1 (NRP1), triggers aberrant branching, migration or growth of the motor neurons in 1-day-old zebrafish embryos (Feldner et al., 2005; Sato-Maeda et al., 2006). Thus, we hypothesized that Pin1 KD could rescue the motor neuron defects induced by reduced Sema3A signaling.

To reduce Sema3A signaling we used morpholinos targeting NRP1 (NRP1-MO) (Lee et al., 2002) and designed specific Pin1 targeting morpholinos. Injection of NRP1 morpholino resulted in 77% reduction of NRP1 level (Fig. 7A, B), and injection of Pin1 targeting morpholino reduced Pin1 level by 53% by western blotting (Fig. 7A, B). Co-injection of NRP1-MO and Pin1-MO resulted in similar reduction of Pin1 and NRP1 as single MO injection (Fig. 7A, line: NRP1 + Pin1 MOs). Next, we analyzed the growth of motor axons in 1-day-old zebrafish embryos using whole mount immunostaining against anti-acetylated tubulin. KD of Pin1 did not significantly affect relative number of zebrafish embryos with defective motor neuron growth (27% vs 17% in control) (Fig. 7C, D). Similarly, the average number of defective axons per embryo (Fig. 7C, D) was also not significantly changed in Pin1-MO embryos (0.40 vs. 0.22 in control). In contrast, NRP1 KD significantly increased number of embryos with aberrant motor neuron growth (85%), with the average of 2.05 defects per embryo (Fig. 7C, D). Importantly, simultaneous KD of NRP1 and Pin1

significantly reduced the relative number of defective embryos (44%) as well as the average of defective motor neuron per embryo (0.95) (Fig. 7C, D), indicating that Pin1 KD partially rescues the motor neuron defects induced by NRP1 KD. Taken together, our data demonstrate that Pin1 regulates Sema3A signaling both *in vitro* and *in vivo*.

DISCUSSION

Using a proteomic approach, we identified CRMP2A as a Pin1 substrate in developing neurons and a regulator of axon growth. Pin1 binds to and stabilizes CRMP2A phosphorylated by CDK5 on the Ser27-Pro motif. As a result, Pin1 KO, KD or inhibition reduces CRMP2A levels primarily in the vicinity of growth cones, where CRMP2A is surprisingly the dominant isoform. Moreover, KO, KD or inhibition of Pin1 results in similar inhibition of axon growth that is fully rescued by overexpression of either Pin1 or CRMP2A. Furthermore, Sema3A but not LPA stimulation drives Pin1 to the vicinity of growth cones where it co-localizes with CRMP2A, and Pin1 KO neurons are more sensitive to Sema3A-induced growth cone collapse by bath or gradient application. Pin1-null mice display in several regions of the peripheral and central nervous system selective developmental axon growth defects, which are associated with reduced CRMP2A, and opposite to those found in Sema3A or Nrp-1 mutant mice. Finally, KD of Pin1 partially rescues developmental defects generated in motor neurons by downregulation of Sema3A signaling. These results not only identify an important isoform-specific function for CRMP2A in regulating axon growth, but also uncover a regulatory mechanism, where Pin1 promotes axon growth by stabilizing CRMP2A selectively in distal axons and buffers low-level Sema3A stimulation.

Regulation of axon growth and collapse by Pin1

Pin1 is so far the only known prolyl isomerase that specifically catalyzes isomerization of Ser/Thr-Pro bonds upon their phosphorylation. Significantly, proline in the pSer/Thr-Pro motif breaks symmetry of the polypeptide chain and makes it prone to conformational changes. Phosphorylation of the motif significantly restrains the spontaneous isomerization of the pSer/Thr-Pro motif and makes it accessible to Pin1, which can then isomerize the motif to acquire a particular conformation, having a major impact on protein function, localization, stability etc. (Lu and Zhou, 2007; Pastorino et al., 2006; Yaffe et al., 1997).

Here we showed that Pin1 binds to and stabilizes CRMP2A in distal axons and that Sema3A stimulation drives Pin1 to the vicinity of growth cones. Thus, the presence of Pin1 in the growth cones might serve as a buffer for Sema3A-induced CDK5 activation and help to maintain an active, intact growth cone till a certain threshold concentration of Sema3A is reached. Consequently, depletion of Pin1 leads to reduced axon growth or premature growth cone collapse. Thus Pin1 level in axons may play an important role in fine-tuning of axon guidance. Importantly, we see that some neuronal projections in Pin1 KO mice (e.g. the ophthalmic branch of the trigeminal nerve) are particularly stunted, less brunched or misguided, whereas other neurons are not affected. Moreover, while the distribution of the phenotypical changes of Pin1 KO neurons follows in many areas (e.g. ophthalmic branch, entorhino-hippocampal projections) the phenotypical pattern of Sema3A KO mice (although

with the opposite effect on the axonal growth), in some regions the patterns are different. E.g. in the developing DRGs, deficiency of Sema3A or Nrp1 leads to a loss of segmentation and increased growth and defasciculation of lateral branches of spinal neurons (Kitsukawa et al., 1997). In Pin1 KO embryos the DRG segmentation is preserved (in agreement with the opposite effects of Pin1 and Sema3A deficiencies; data not shown), but the growth of the spinal nerves is more variable. While lateral branches of spinal nerves showed reduced growth in the cervical area (Fig. 6F–H, two out of four Pin1 KO, none out of five Pin1 WT embryos), the innervation of forelimbs, which is also defasciculated in Sema3A or Nrp1 deficient mice, was not affected in Pin1 KO mice (none of 4 Pin1 KO embryos, not shown). The discrepancy indicates that Pin1-KO phenotype is not simply the opposite of the Sema3A-KO or NRP1-KO mice in every part of the developing nervous system. This could be due to either, different ability of various neurons to compensate for Pin1 deficiency (e.g. by other, non-phospho-specific isomerases), or by other members of the CRMP family rescuing the CRMP2A insufficiency, all resulting in a different vulnerability of different neurons to Pin1 deficiency. Consistent with this hypothesis, we found that the levels of Pin1 in distal DRG axons in vitro are highly variable, and correlating with CRMP2A levels (Fig. 5A). These results indicate that expression and/or distribution of Pin1 in the growing DRG axons is regulated, giving some neurons growth advantage in Sema3A rich environment and at the same time making these neurons more vulnerable to Pin1 deficiency. Similarly it has been shown in human and mouse, that various levels of Pin1 expression in different brain regions inversely correlate with their vulnerability to neurofibrillary degeneration in AD (Liou et al., 2003).

In order to test genetic interaction between Sema3A signaling and Pin1 in vivo we utilized the model of motor neuron development in zebrafish. It has been shown before, that downregulation of Sema3A signaling results in defective growth of motor neurons (Feldner et al., 2005; Sato-Maeda et al., 2006). Interestingly, KD of Sema3A homologues in zebrafish produced contradictory results as for their effect on motor neuron growth, likely due to compensation by other Sema3A homologue (zebrafish has two) or by other guidance/ signaling molecules. For this reason, in order to silence Sema3A signaling in motor neurons, we chose KD of Nrp1, which has been reproducibly shown to induce motor neuron growth defects (Feldner et al., 2005; Sato-Maeda et al., 2006). Nrp1, though, has also been shown to serve also as VEGF receptor (Gu et al., 2003), indicating that by knocking down Nrp1 we also interfere with the VEGF pathway. Importantly, in zebrafish VEGF KD has been shown *per se* not to induce significant motor neuron defects in motor neurons, while it did have a clear effect on vascular development (Feldner et al., 2005). Thus while VEGF could play a minor role in the Pin1 rescue experiments in zebrafish, the major effect was via Sema3A signaling.

Based on our data, we propose a model for the role of Pin1 in regulating Sema3Adriven axonal growth/retraction (Fig. 7E–H). In absence of Sema3A, CRMP2A present in distal axons is not phosphorylated, promoting tubulin assembly and axon growth in both Pin1 WT and KO neurons (Fig. 7E). Low levels of Sema3A stimulation activate CDK5, which phosphorylates CRMP2A at Ser27 and Ser623, attracting Pin1 to the vicinity of the growth cones where it binds and stabilizes phosphorylated CRMP2A (Fig. 7F). In the dynamic

equilibrium between phosphorylation and dephosphorylation, Pin1-dependent stabilization of phoshpo-CRMP2A sustains the pool of active CRMP2A in the growth cone. In the absence of Pin1, low levels of CRMP2A phosphorylation eventually deplete the growth cone of the active CRMP2A pool, which shifts the dynamic microtubule equilibrium towards growth cone collapse. In the presence of high levels of Sema3A (Fig. 7G), activated CDK5 and GSK-3β hyperphosphorylate CRMP2A to reduce its affinity for tubulin heterodimers, leading to growth cone collapse in both Pin1 WT and KO neurons. Reduction of Sema3A signaling (e.g. by KD of NRP1) (Fig. 7H) triggers aberrant growth of axons in Sema3A gradients, but simultaneous KD of Pin1 increases sensitivity to Sema3A signaling and partially rescues the defective growth of NRP1 KD axons.

Experimental procedures

Detailed description of experimental procedures is present in the Supplemental Information.

Animals

All experimental procedures were performed in compliance with animal protocols approved by the Institutional Animal Care and Use Committee at Beth Israel Deaconess Medical Center. Zebrafish were mated, staged, and raised as described (Westfield, 2000) in accordance with IACUC guidelines,

GST pulldown assays and co-immunoprecipitations

GST pulldown, immunoprecipitation, and immunoblotting analyses were performed as described (Lu et al., 1999b; Yaffe et al., 1997) using SH-SY5Y or HEK293T cell lysates incubated with either GST or GST-Pin1 or a specific antibody and then glutathione agarose beads or protein Agarose, followed by washing elution and western blotting analysis.

Histology, immunohistochemistry and immunocytochemistry

Histology, immunohistochemistry, immunocytochemistry and quantificaiton were carried out as described previously (Lee et al., 2009; Liou et al., 2003; Pastorino et al., 2006). Briefly, mice were intracardially perfused with PBS and ice-cold fixative solution (4% paraformaldehyde (PFA) in PBS), embedded in paraplast and 8 μm thick horizontal sections were cut. For immunohistochemistry sections were incubated with primary antibodies in PBS with 10% FCS and 0.2% Tween 20 overnight at 4 °C and washed three times for 10 min with 0.2% Tween 20 in PBS. Secondary antibodies were then applied and incubated for 1 h at room temperature, washed twice with 0.2% Tween/PBS and embedded in Mowiol with 1 μg/ml DAPI. Whole-mount immunohistochemistry of E12.5 embryos was performed as described (Klymkowsky and Hanken, 1991). Briefly, embryos were fixed with 4% paraformaldehyde in PBS overnight at 4 °C and soaked in 80% methanol. Endogenous peroxidase activity was quenched with 3% H_2O_2 in Dent's fixative (80% methanol and 20%dimethylsulfoxide) for 3 hr, embryos were washed with PBS with 1% Tween 20, and incubated with the anti-neurofilament antibody clone 2H3 (1:100) for 2 days at room temperature. Detection of 2H3 was performed with Vectastain ABC elite kit, (Vector). HRP activity was detected with diaminobenzidine. For immunocytochemistry cells grown on poly-D lysine (Invitrogen) and laminin (BD bioscience) coated coverslips were fixed in ice

cold 4%PFA/PBS for 15 min, and methanol (–20 °C, 6 min), washed in PBS and incubated with primary antibodies overnight at 4 °C. Fluorescence secondary antibodies were then applied and incubated for 1 h at room temperature, washed twice with PBS and embedded in Mowiol with 0.5 μg/ml DAPI. Fluorescent images were taken using a confocal microscope (Zeiss, LSM510), and outlines were generated using ImageJ software. For quantification of total CRMP2 vs. CRMP2A levels upon CRMP2A or Pin1 knockdown, a median signal intensity was measured in each soma and axon shaft of all neurons within at least 4 randomly picked optical fields using ImageJ software. Mean relative values ± SEM were then calculated for either of the two neuron parts in all experimental conditions. Phase contrast microscopy images were taken using Nikon eclipse TS100.

S1 neuron anterograde tracing was performed in 4 months old Pin1 KO and Pin1 WT animals by inserting carbocyanide dye DiI crystals into the 4%PFA fixed brains, S1 region as described previously (Niquille et al., 2009). The DiI was let penetrating 3–4 weeks in 4%PFA/PBS at 37°C. 100μm coronal brains sections were cut on vibratome (Leica), images taken using Nikon eclipse TS100 and Leica SP8 microscopes, and analyzed by ImageJ software.

Axon length and indirect CRMP2A/B content measurement

Primary neurons transduced with lentiviral vectors or treated with Juglone were fixed at 4 DIV and immunostained for MAP2 (dendritic) and tau (axonal) markers. The length of the longest neurite showing specific tau but no MAP2 signal was traced and measured as that of an axon using NeuroJ software. Axon length of neurons in at least 2 randomly selected optical fields and at least 50 neurons in total were counted for each construct and mean axon length ± SEM was calculated. In Pin1 KO rescue experiments, neurons co-transfected with GFP and FLAG-CRMP2A (or empty vector) were fixed at 7 DIV and co-immunostained for βIII tubulin to distinguish primary neurons and FLAG, to visualize distribution of FLAG-CRMP2A in the neurons. The length of the longest neurite showing (in the FLAG-CRMP2A transfected neurons) specific CRMP2A localization close to the growth cones, was traced and measured as that of an axon at 7 DIV using NeuronJ plugin of ImageJ software.

For indirect measurement of CRMP2A/B levels, the median intensity of CRMP2A and total CRMP2(A+B) were measured in the axon shafts using ImageJ software in primary cortical cultures at 4DIV (3 days after infection with silencing or control lentiviral vectors), with the longest neurite considered as axon. Average CRMP2A and total CRMP2(A+B) intensity of axons from at least 3 optical fields was calculated and used to quantify the relative CRMP2A/B levels.

Morpholino KD in zebrafish

Morpholinos targeting NRP1 and Pin1 were synthesized by Gene Tools (Philomath, OR) and injected into one to two-cell stage embryos. 1-day-old zebrafish embryos were immunostained using acetylated-tubulin antibodies (Sigma) and analyzed.

Cell cultures, transfection and infection

Human neuroblastoma SH-SY5Y and human embryonic carcinoma HEC293T cell lines were cultured in DMEM with 10% FCS and transfected using PEI 25 kDa, linear (Polysciences Inc., 1 µg/ml in H_2O). Primary cortical neurons were prepared and cultured as described (Nikolic et al., 1996). Briefly, cortices were dissected from E15.5 embryonic brains in HBSS (Invitrogen) supplemented with 20mM HEPES pH 7.3. Cells were dissociated with trypsin, plated on to laminin and poly-D-lysine-coated glass coverslips and maintained in neurobasal media supplemented with factor B27 (Invitrogen) and 2 mM L-glutamine (Invitrogen). Primary neuron transfection was performed 1 day after plating using Lipofectamin 2000 (Invitrogen) as described elsewhere (Ohki et al., 2001).

pLKO.1 lentiviral vector (Open biosystems) was used for gene silencing experiments with following target sequences: human Sh-Pin1 CCACCGTCACACAGTATTTAT; mouse Sh-Pin1 CCGGGTGTACTACTTCAATCA; Non-silencing control ATCTCGCTTGGGCGAGAGTAAG and Sh-CRMP2A TGGAAGGGTCCTCGGAGAA. For lentiviral overexpression FLAG-Pin1 was subcloned into pLenti6/V5-GW/lacZ vector (Invitrogen). HEK293T cells were cotransfected with lentiviral construct, a Gag-Pol construct and a VSV-G envelope construct using PEI. Virus containing supernatants was collected at 48 and 72 hours after transfection, filtered though 0.45-µm filter, and concentrated using a Centricon Plus-70 100000 MWCO column (Millipore). Primary neurons were infected 18 h after plating, 4 h after infection the media was replaced and infected neurons were selected 1.5 days after infection with 1 µg/ml puromycin.

Pin1 inhibition in primary cortical neurons was performed 1 day after plating by adding 4µM Juglone into the media.

Compartmented chamber cultures were prepared from rat E15.5 DRG neurons.

Statistics

Student's T-test and nonparametric Man-Whitney test were used to determine the statistical significance of the experimental results.

Supplementary Material

Refer to Web version on PubMed Central for supplementary material.

Acknowledgements

References

Arimura N, Inagaki N, Chihara K, Menager C, Nakamura N, Amano M, Iwamatsu A, Goshima Y, Kaibuchi K. Phosphorylation of collapsin response mediator protein-2 by Rho-kinase. Evidence for two separate signaling pathways for growth cone collapse. J Biol Chem. 2000; 275:23973–23980. [PubMed: 10818093]

Arimura N, Menager C, Kawano Y, Yoshimura T, Kawabata S, Hattori A, Fukata Y, Amano M, Goshima Y, Inagaki M, et al. Phosphorylation by Rho kinase regulates CRMP-2 activity in growth cones. Mol Cell Biol. 2005; 25:9973–9984. [PubMed: 16260611]

Balastik M, Lim J, Pastorino L, Lu KP. Pin1 in Alzheimer's disease: multiple substrates, one regulatory mechanism? Biochim Biophys Acta. 2007; 1772:422–429. [PubMed: 17317113]

Behar O, Golden JA, Mashimo H, Schoen FJ, Fishman MC. Semaphorin III is needed for normal patterning and growth of nerves, bones and heart. Nature. 1996; 383:525–528. [PubMed: 8849723]

Cole AR, Knebel A, Morrice NA, Robertson LA, Irving AJ, Connolly CN, Sutherland C. GSK-3 phosphorylation of the Alzheimer epitope within collapsin response mediator proteins regulates axon elongation in primary neurons. J Biol Chem. 2004; 279:50176–50180. [PubMed: 15466863]

Culotti JG, Kolodkin AL. Functions of netrins and semaphorins in axon guidance. Curr Opin Neurobiol. 1996; 6:81–88. [PubMed: 8794052]

Deller T, Adelmann G, Nitsch R, Frotscher M. The alvear pathway of the rat hippocampus. Cell Tissue Res. 1996; 286:293–303. [PubMed: 8929332]

Feldner J, Becker T, Goishi K, Schweitzer J, Lee P, Schachner M, Klagsbrun M, Becker CG. Neuropilin-1a is involved in trunk motor axon outgrowth in embryonic zebrafish. Dev Dyn. 2005; 234:535–549. [PubMed: 16110501]

Fukata Y, Itoh TJ, Kimura T, Menager C, Nishimura T, Shiromizu T, Watanabe H, Inagaki N, Iwamatsu A, Hotani H, et al. CRMP-2 binds to tubulin heterodimers to promote microtubule assembly. Nat Cell Biol. 2002; 4:583–591. [PubMed: 12134159]

Gu C, Rodriguez ER, Reimert DV, Shu T, Fritzsch B, Richards LJ, Kolodkin AL, Ginty DD. Neuropilin-1 conveys semaphorin and VEGF signaling during neural and cardiovascular development. Dev Cell. 2003; 5:45–57. [PubMed: 12852851]

Gu Y, Hamajima N, Ihara Y. Neurofibrillary tangle-associated collapsin response mediator protein-2 (CRMP-2) is highly phosphorylated on Thr-509, Ser-518, and Ser-522. Biochemistry. 2000; 39:4267–4275. [PubMed: 10757975]

Hennig L, Christner C, Kipping M, Schelbert B, Rucknagel KP, Grabley S, Kullertz G, Fischer G. Selective inactivation of parvulin-like peptidyl-prolyl cis/trans isomerases by juglone. Biochemistry. 1998; 37:5953–5960. [PubMed: 9558330]

Inagaki N, Chihara K, Arimura N, Menager C, Kawano Y, Matsuo N, Nishimura T, Amano M, Kaibuchi K. CRMP-2 induces axons in cultured hippocampal neurons. Nat Neurosci. 2001; 4:781–782. [PubMed: 11477421]

Kitsukawa T, Shimizu M, Sanbo M, Hirata T, Taniguchi M, Bekku Y, Yagi T, Fujisawa H. Neuropilin-semaphorin III/D-mediated chemorepulsive signals play a crucial role in peripheral nerve projection in mice. Neuron. 1997; 19:995–1005. [PubMed: 9390514]

Klymkowsky MW, Hanken J. Whole-mount staining of Xenopus and other vertebrates. Methods Cell Biol. 1991; 36:419–441. [PubMed: 1725802]

Lee P, Goishi K, Davidson AJ, Mannix R, Zon L, Klagsbrun M. Neuropilin-1 is required for vascular development and is a mediator of VEGF-dependent angiogenesis in zebrafish. Proc Natl Acad Sci U S A. 2002; 99:10470–10475. [PubMed: 12142468]

Lee TH, Tun-Kyi A, Shi R, Lim J, Soohoo C, Finn G, Balastik M, Pastorino L, Wulf G, Zhou XZ, et al. Essential role of Pin1 in the regulation of TRF1 stability and telomere maintenance. Nat Cell Biol. 2009; 11:97–105. [PubMed: 19060891]

Liou YC, Sun A, Ryo A, Zhou XZ, Yu ZX, Huang HK, Uchida T, Bronson R, Bing G, Li X, et al. Role of the prolyl isomerase Pin1 in protecting against age-dependent neurodegeneration. Nature. 2003; 424:556–561. [PubMed: 12891359]

Lu KP, Finn G, Lee TH, Nicholson LK. Prolyl cis-trans isomerization as a molecular timer. Nat Chem Biol. 2007; 3:619–629. [PubMed: 17876319]

Lu KP, Zhou XZ. The prolyl isomerase PIN1: a pivotal new twist in phosphorylation signalling and disease. Nat Rev Mol Cell Biol. 2007; 8:904–916. [PubMed: 17878917]

Lu PJ, Wulf G, Zhou XZ, Davies P, Lu KP. The prolyl isomerase Pin1 restores the function of Alzheimer-associated phosphorylated tau protein. Nature. 1999a; 399:784–788. [PubMed: 10391244]

Lu PJ, Zhou XZ, Liou YC, Noel JP, Lu KP. Critical role of WW domain phosphorylation in regulating phosphoserine binding activity and Pin1 function. J Biol Chem. 2002; 277:2381–2384. [PubMed: 11723108]

Lu PJ, Zhou XZ, Shen M, Lu KP. Function of WW domains as phosphoserine- or phosphothreonine-binding modules. Science. 1999b; 283:1325–1328. [PubMed: 10037602]

Nakamura K, Greenwood A, Binder L, Bigio EH, Denial S, Nicholson L, Zhou XZ, Lu KP. Proline isomer-specific antibodies reveal the early pathogenic tau conformation in Alzheimer's disease. Cell. 2012; 149:232–244. [PubMed: 22464332]

Nikolic M, Dudek H, Kwon YT, Ramos YF, Tsai LH. The cdk5/p35 kinase is essential for neurite outgrowth during neuronal differentiation. Genes Dev. 1996; 10:816–825. [PubMed: 8846918]

Niquille M, Garel S, Mann F, Hornung JP, Otsmane B, Chevalley S, Parras C, Guillemot F, Gaspar P, Yanagawa Y, et al. Transient neuronal populations are required to guide callosal axons: a role for semaphorin 3C. PLoS Biol. 2009; 7:e1000230. [PubMed: 19859539]

Ohki EC, Tilkins ML, Ciccarone VC, Price PJ. Improving the transfection efficiency of post-mitotic neurons. J Neurosci Methods. 2001; 112:95–99. [PubMed: 11716945]

Pastorino L, Sun A, Lu PJ, Zhou XZ, Balastik M, Finn G, Wulf G, Lim J, Li SH, Li X, et al. The prolyl isomerase Pin1 regulates amyloid precursor protein processing and amyloid-beta production. Nature. 2006; 440:528–534. [PubMed: 16554819]

Pazyra-Murphy MF, Segal RA. Preparation and maintenance of dorsal root ganglia neurons in compartmented cultures. J Vis Exp. 2008

Pozas E, Pascual M, Nguyen Ba-Charvet KT, Guijarro P, Sotelo C, Chedotal A, Del Rio JA, Soriano E. Age-dependent effects of secreted Semaphorins 3A, 3F, and 3E on developing hippocampal axons: in vitro effects and phenotype of Semaphorin 3A (–/–) mice. Mol Cell Neurosci. 2001; 18:26–43. [PubMed: 11461151]

Quinn CC, Chen E, Kinjo TG, Kelly G, Bell AW, Elliott RC, McPherson PS, Hockfield S. TUC-4b, a novel TUC family variant, regulates neurite outgrowth and associates with vesicles in the growth cone. J Neurosci. 2003; 23:2815–2823. [PubMed: 12684468]

Sasaki Y, Cheng C, Uchida Y, Nakajima O, Ohshima T, Yagi T, Taniguchi M, Nakayama T, Kishida R, Kudo Y, et al. Fyn and Cdk5 mediate semaphorin-3A signaling, which is involved in regulation of dendrite orientation in cerebral cortex. Neuron. 2002; 35:907–920. [PubMed: 12372285]

Sato-Maeda M, Tawarayama H, Obinata M, Kuwada JY, Shoji W. Sema3a1 guides spinal motor axons in a cell- and stage-specific manner in zebrafish. Development. 2006; 133:937–947. [PubMed: 16452100]

Schmidt EF, Strittmatter SM. The CRMP family of proteins and their role in Sema3A signaling. Adv Exp Med Biol. 2007; 600:1–11. [PubMed: 17607942]

Tessier-Lavigne M, Goodman CS. The molecular biology of axon guidance. Science. 1996; 274:1123–1133. [PubMed: 8895455]

Uchida Y, Ohshima T, Sasaki Y, Suzuki H, Yanai S, Yamashita N, Nakamura F, Takei K, Ihara Y, Mikoshiba K, et al. Semaphorin3A signalling is mediated via sequential Cdk5 and GSK3beta phosphorylation of CRMP2: implication of common phosphorylating mechanism underlying axon guidance and Alzheimer's disease. Genes Cells. 2005; 10:165–179. [PubMed: 15676027]

Westfield, M. A guide for the laboratory use of zebrafish (Danio rerio). 4th ed.. Eugene: Univ of Oregon Press; 2000. The Zebrafish Book.

White FA, Behar O. The development and subsequent elimination of aberrant peripheral axon projections in Semaphorin3A null mutant mice. Dev Biol. 2000; 225:79–86. [PubMed: 10964465]

Yaffe MB, Schutkowski M, Shen M, Zhou XZ, Stukenberg PT, Rahfeld JU, Xu J, Kuang J, Kirschner MW, Fischer G, et al. Sequence-specific and phosphorylation-dependent proline isomerization: a potential mitotic regulatory mechanism. Science. 1997; 278:1957–1960. [PubMed: 9395400]

Yoshimura T, Kawano Y, Arimura N, Kawabata S, Kikuchi A, Kaibuchi K. GSK-3beta regulates phosphorylation of CRMP-2 and neuronal polarity. Cell. 2005; 120:137–149. [PubMed: 15652488]

Yuasa-Kawada J, Suzuki R, Kano F, Ohkawara T, Murata M, Noda M. Axonal morphogenesis controlled by antagonistic roles of two CRMP subtypes in microtubule organization. Eur J Neurosci. 2003; 17:2329–2343. [PubMed: 12814366]

Zhou J, Wen Y, She L, Sui YN, Liu L, Richards LJ, Poo MM. Axon position within the corpus callosum determines contralateral cortical projection. Proc Natl Acad Sci U S A. 2013; 110:E2714–E2723. [PubMed: 23812756]
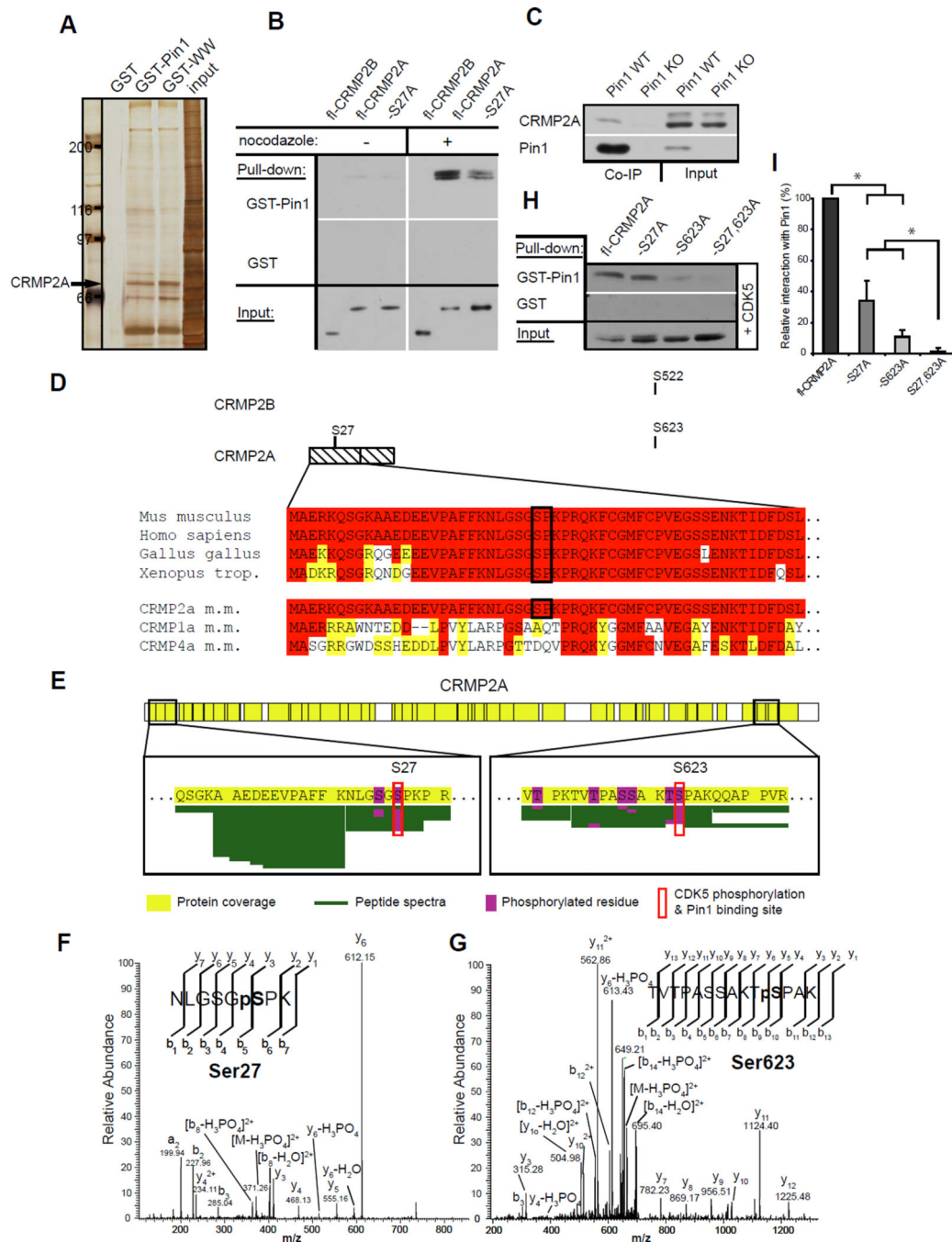
Figure 1. Proteomic identification of CRMP2A as a major Pin1-binding protein in the nervous system

(A) Silver staining of proteins pulled down from postnatal mouse brain lysates by Pin1 (GST-Pin1), its WW-domain (GST-WW) or control GST. CRMP2A band identified by tandem Mass spectrometry indicated. (B) Pin1 binding to mitotically phosphorylated CRMP2A. SH-SY5Y cells expressing FLAG-CRMP2A (fl-CRMP2A) or its S27A mutant (-S27A) were untreated or treated with Nocodazole, followed by pulldown assay with GST-Pin1 (upper panels) or control GST (middle panels). (C) Endogenous Pin1 and CRMP2A form stable complexes in the brain. Pin1 WT and KO brain lysates were subjected to Co-IP

with anti-Pin1 antibodies, followed by immunoblotting with anti-CRMP2A antibodies. (D) CRMP2A differs from CRMP2B due to the presence of a 114 long amino acid long N-terminal sequence containing a single Pin1 binding/CDK5 phosphorylation site at Ser27. The site is highly conserved among species but is not present in other CRMP family members that have longer forms. (E–G) Tandem mass spectrometry detected phosphorylation of Ser27 and Ser623 in FLAG-CRMP2A pulled down by Pin1 from HEK-293T cells cotransfected with FLAG-CRMP2A and CDK5/p25 (E). Underlining green lines represent peptide sequence coverage and phosphorylation modifications are highlighted in magenta. The MS/MS spectra are shown for phosphorylation of Ser27 (F) and Ser623 (G). (H) Ala substitution of either Ser27 (-S27A), or Ser623 (-S623A) reduced, but Ala substitution of both sites completely abolishes binding to Pin1. SH-SY5Y cells were cotransfected with FLAG-CRMP2A or its mutants and p25/CDK5, followed by GST-Pin1 pulldown assay. (I) Quantification of Pin1 binding to various CRMP2A mutants. See also Figure S1.
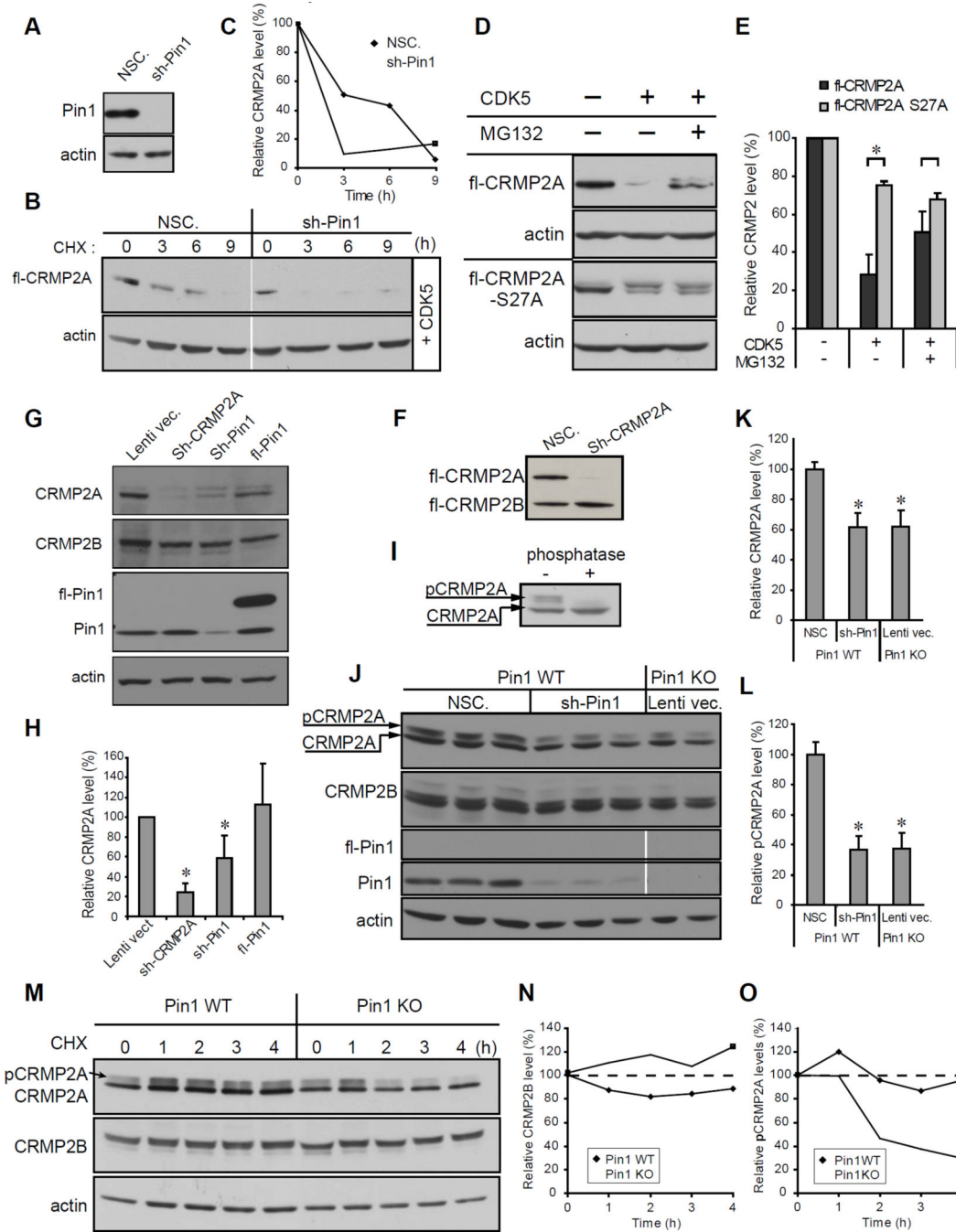
Figure 2. Pin1 stabilizes CRMP2A phosphorylated by CDK5

(A–C) Pin1 KD reduces stability of transfected CRMP2A. SH-SY5Y cells were stably infected with Pin1 silencing (Sh-Pin1) or non-silencing (NSC) lentiviruses (A), and then co-transfected with FLAG-CRMP2A (fl-CRMP2A) and p25/Cdk5, followed by cycloheximide (CHX) chase to measure CRMP2A stability (B) with semi-quantitative results of CRMP2A levels shown in (C). (D) Phosphorylation of CRMP2A on Ser27 by CDK5 increases protein turnover. HEK-293T cells were transfected with fl-CRMP2A or its Ser27Ala mutant with or without p25/Cdk5 in the absence or presence of MG132, followed by immunoblotting with

anti-FLAG antibodies (E). (F) Sh-CRMP2A silences CRMP2A but not CRMP2B. SH-SY5Y cells were infected with Sh-CRMP2A lentiviruses, followed by immunoblotting analysis. (G) KD of CRMP2A or Pin1 significantly reduces endogenous CRMP2A but not CRMP2B. SH-SY5Y cells were infected with lentiviruses expressing CRMP2A, Sh-Pin1, or full length Pin1 (Sh-CRMP2A, Sh-Pin1 or fl-Pin1), followed by immunoblotting analysis (H). (I) Incubation with λ phosphatase identifies CRMP2A mobility shift caused by phosphorylation. Primary cortical neuron lysates were incubated without or with λ phosphatase followed by immunoblotting analysis, identifying phosphorylated CRMP2A (pCRMP2A). (J–L) Pin1 KD reduces CRMP2A to levels detected in Pin1-KO cells without affecting CRMP2B in primary neurons. Primary cortical neuron cultures derived from 3 different Pin1 WT embryos and 2 Pin1 KO embryos at E15.5 were infected with Sh-Pin1 lentiviruses, NSC control or lentiviral vector control, followed by immunoblotting analysis (J) with semi-quantification of total (K) or phosphorylated (L) CRMP2A and CRMP2A levels normalized to CRMP2B. (M) Pin1 KO reduces stability of endogenous phosphorylated CRMP2A in primary neurons. Cycloheximide chase was performed on primary cortical neurons at 6DIV with semi-quantitative results of CRMP2B and phospho-CRMP2a levels shown in (N) and (O) respectively (means ± S.D. values shown; * $p < 0.05$).
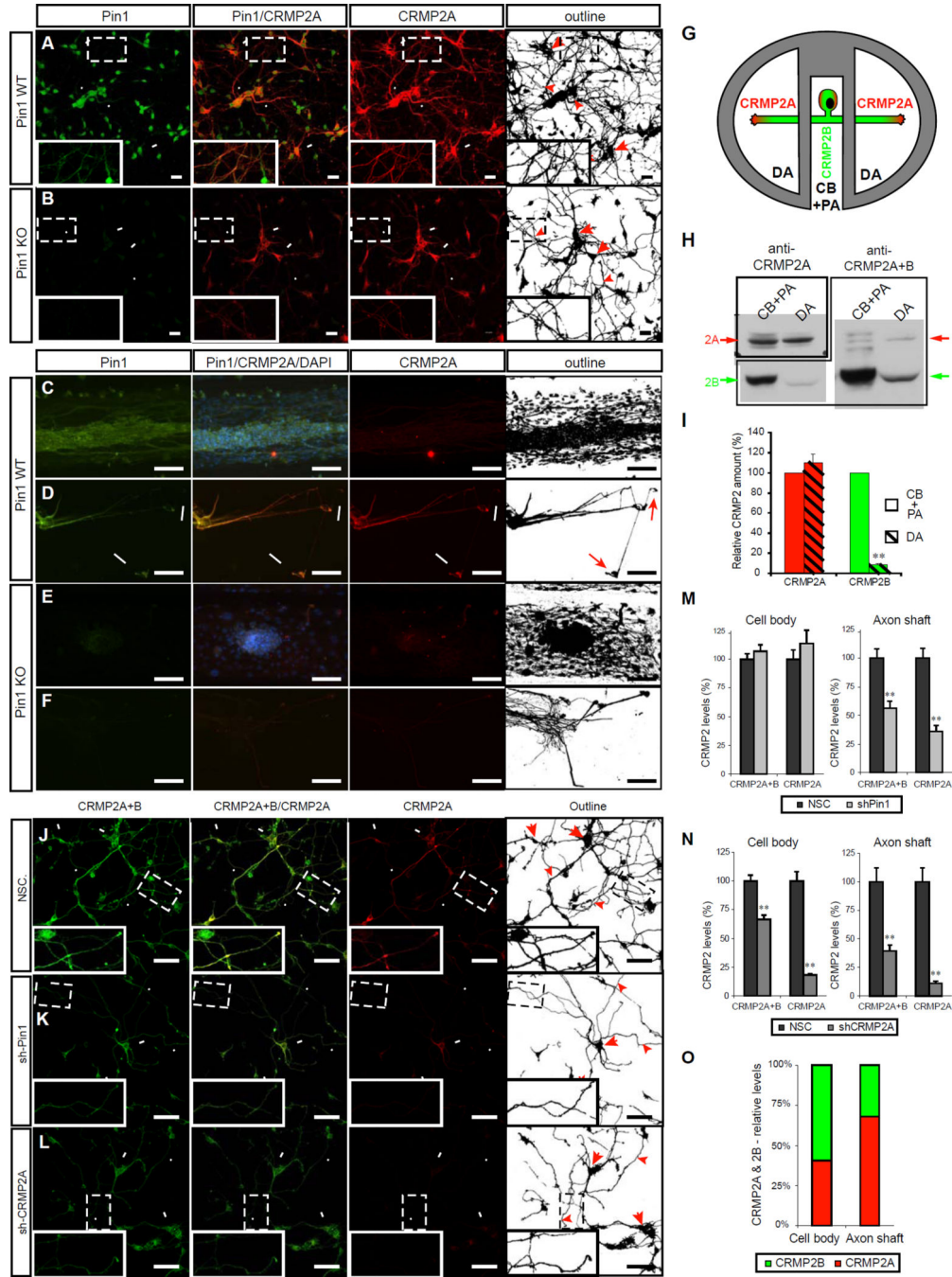
Figure 3. Pin1 stabilizes CRMP2A selectively in the distal neurites of primary neurons
(A, B) Pin1 KO reduces CRMP2A selectively in the distal neurites of primary neurons. CRMP2A (red) and Pin1 (Green) immunostaining in Pin1 WT and KO primary cortical neurons at 3 DIV. (A) CRMP2A is expressed strongly in the soma (arrows) as well in the neurites (arrowheads) and co-localize with Pin1 in the neurites (insets). In the Pin1 KO neurons (B), CRMP2A level is lower in the neurites (arrowheads), but its levels in the somas are comparable to WT (arrows). (C–F) Pin1 KO reduces CRMP2A in axons. Using rat Pin1 WT DRG compartmental cultures, Pin1 was detected both in the cell body + proximal axon

(CB+PA) compartment (C), as well as in distal axons (DA) (D) by double immunostaining, while higher expression of CRMP2A (co-localizing with Pin1) was detected in DA close to growth cones (D, arrows) when compared to the CB+PA (C). In the Pin1 KO DRG neurons, CRMP2A expression in the DA (F), but not in the CB+PA region (E), is significantly reduced. (G–I) Relative level of CRMP2A increases in distal axon region. Lysates collected from DA and CB+PA compartments of rat primary DRG compartment cultures (G) were analyzed by western blotting using CRMP2A and total CRMP2A+B antibodies (H). Semi-quantitative analysis of the CRMP2A and B levels shows significant reduction of CRMP2B levels in distal axons while no significant reduction of CRMP2A (I). (J–L) Pin1 KD reduces CRMP2A and total CRMP2 selectively in the neurites. Pin1 WT primary cortical neurons were infected with non-silencing (NSC), Sh-Pin1 or Sh-CRMP2A lentiviruses, and immunostained for CRMP2A (red) or total CRMP2 (CRMP2A+B) (Green). In NSC neurons, high levels of CRMP2A and total CRMP2 (CRMP2A+B) were detected both in the neurites (arrowhead) and the soma (arrow) (J). Pin1 KD significantly reduced CRMP2A and total CRMP2 levels in neurites (arrowhead) but not in cell bodies (arrow) (K). CRMP2A KD significantly decreases CRMP2A and total CRMP2 levels in neurites (arrowhead) as well as cell bodies (arrows) (L). (M, N) Quantification of total CRMP2 and CRMP2A levels in Pin1 KD (shPin1) and non-silencing shRNA (NSC) control neurons in neuronal cell body and in the axon shafts (M). (O) Quantification of total CRMP2B and CRMP2A levels in CRMP2A KD (shCRMP2A) and control (NSC) neurons in neuronal cell body and in the axon shafts. (O) Relative distribution of CRMP2A vs. CRMP2B in the cell body and in distal axons calculated from (N). (Scale bars: A, B 20μm ; C-F, J-L 50μm). (means ± SEM; ** p< 0.0001)
See also Figure S2.
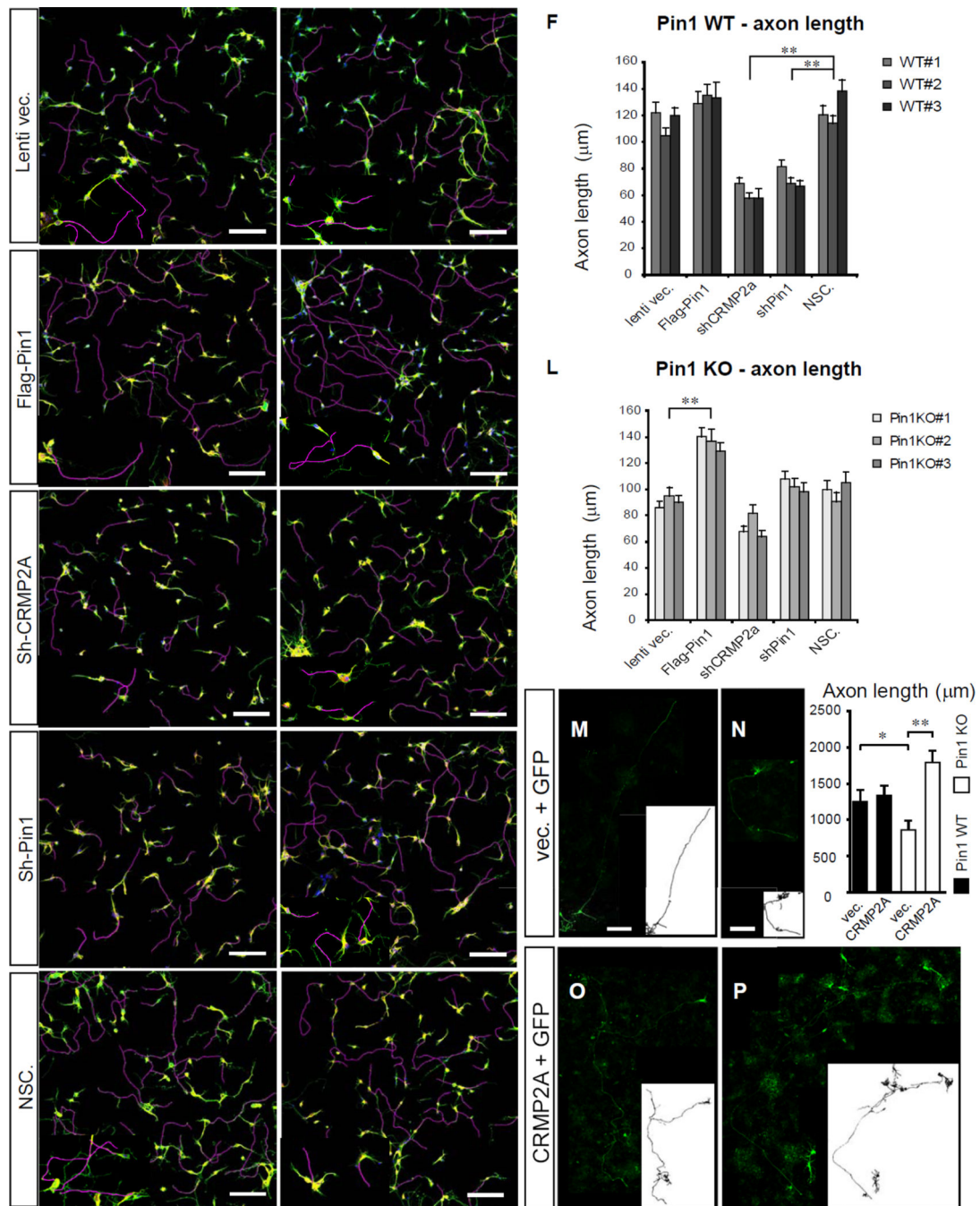
Figure 4. KD/KO of Pin1 reduces axon growth in primary neurons and is fully rescued by CRMP2A overexpression

Primary cortical neuron cultures were derived from embryos of 3 independent Pin1 WT (A–F) and KO (G–L) mouse littermates and infected with lentiviruses expressing control vector (A, G), Flag-Pin1 (B, H), Sh-CRMP2A (C, I), Sh-Pin1 (D, J), or non-silencing shRNA (NSC) (E, K) lentiviruses. Their axon length was determined at 3 DIV by immunostaining for an axon marker tau (green) and a dendrite marker MAP2 (yellow). Axon tracings are shown in violet. (F) and (L) show the means ± SEM values calculated from quantification of at least 2 optical fields and at least 50 neurons total per each experiment. In Pin1 WT

neurons, while overexpression of Pin1 did not have significant effects, KD of CRMP2A or Pin1 in Pin1 WT neurons significantly reduced axon length (** $p < 0.0001$). In Pin1 KO neurons, overexpression of Pin1 completely rescued axon length, but KD of CRMP2A or Pin1 did not significantly reduce axon length, although Sh-CRMP2A neurons had slightly shorter axon. (M-P) CRMP2A overexpression fully rescues shortened axon length in Pin1 KO neurons. Pin1 WT (M, O) and KO (N, P) primary cortical neurons were co-transfected with GFP and vector control (M, N) or GFP and FLAG-CRMP2A (O, P) and axon growth was analyzed at 7 DIV in GFP-positive neurons. Outlines of the neurons are shown in lower right boxes. Upper right panel indicates quantification of the axon lengths as mean ± SEM. (* $p < 0.05$, ** $p < 0.001$), (Scale bars: 100μm) See also Figure S3.
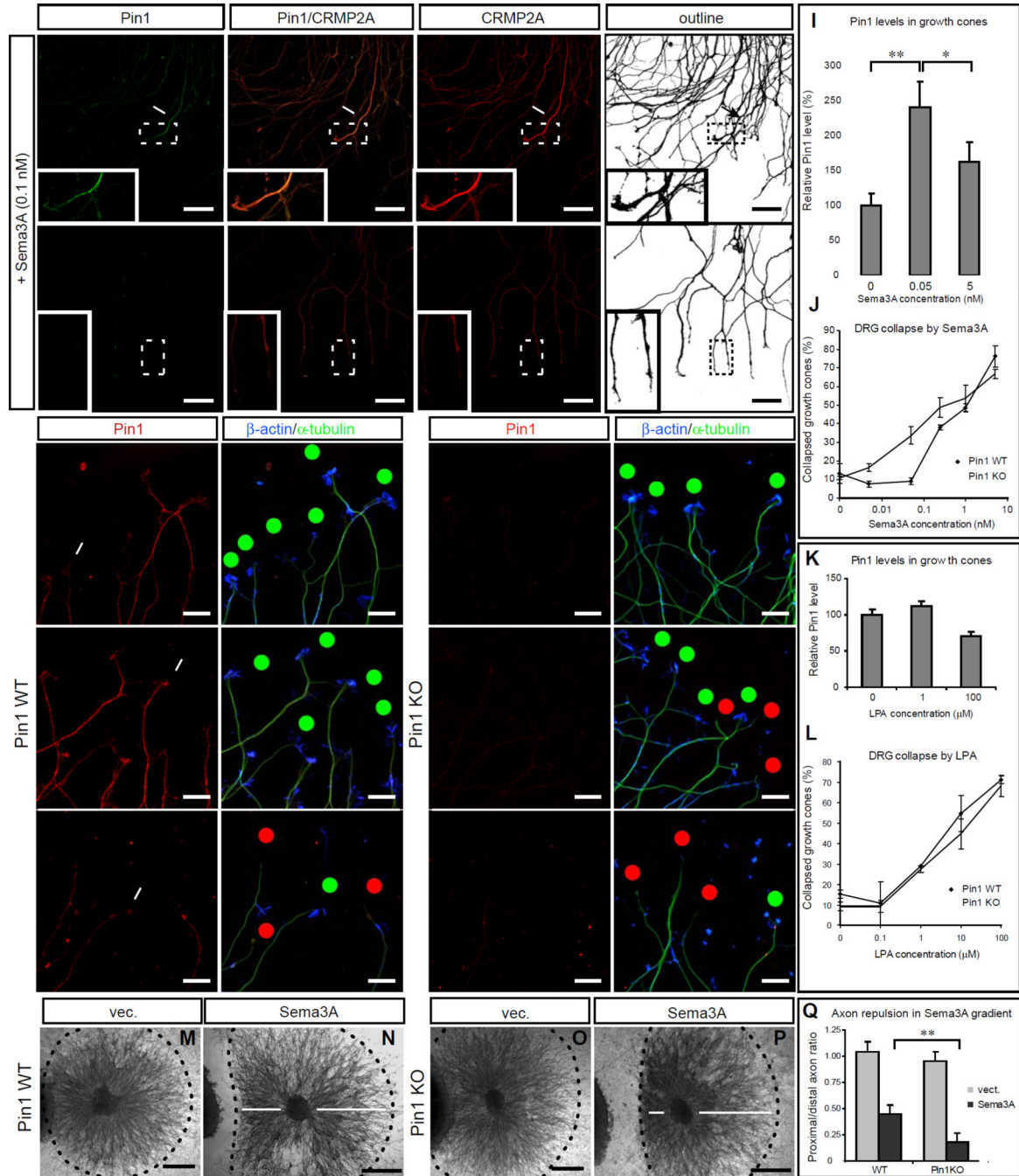
Figure 5. Pin1 KO increases sensitivity to Sema3A-induced growth cone collapse in primary dorsal root ganglia (DRG) neurons

(A, B) Sema3A induces colocalization of high levels of Pin1 and CRMP2A in the vicinity of growth cones (arrows) in Pin1 WT, but not Pin1 KO DRG axons. Pin1 WT (A) and KO (B) primary DRG neurons were treated with 0.1 nM Sema3A for 30 min, followed by double immunostaining for Pin1 (green) and CRMP2A (red). (C–H) Pin1 KO increases sensitivity to Sema3A-induced growth cone collapse. Pin1 WT (C–E) and KO (F–H) primary DRG neurons were treated with different concentrations of Sema3A for 30 min, fixed and triple immunostained with anti Pin1, β-actin and β-tubulin antibodies followed by growth cone

collapse analysis, with the percentage of growth cone collapse being shown in (J) Red dots – collapsed growth cones; green dots – intact growth cones. Intensity of Pin1 immunostaining in DRG growth cones (C) significantly increases upon low (non-collapsing) Sema3A stimulation (D) and is reduced upon high Sema3A stimulation (E); the quantification after normalization to β-tubulin levels is shown (I). (K, L) Stimulation with LPA induces similar growth cone collapse in Pin1 WT and KO DRG neurons (L) and does not affect Pin1 levels in the growth cones (K). (M–Q) Pin1 KO significantly increases sensitivity to Sema3A induced growth cone collapse in collagen 3D co-cultures. SH-SY5Y cells were transfected with empty vector (m, o) or Sema3A expression vector (N, P), and co-cultured with Pin1 WT (M, N) or KO (O, P) DRGs. Distance of the collapsed axons from the gradient source was measured (n, p arrows) upon NF-M immunostaining and quantified (Q) (Scale bars: A,B 50μm, C–H 20μm; , M–P 500μm; * p< 0.05; ** p<0.0001).

See also Figure S4.
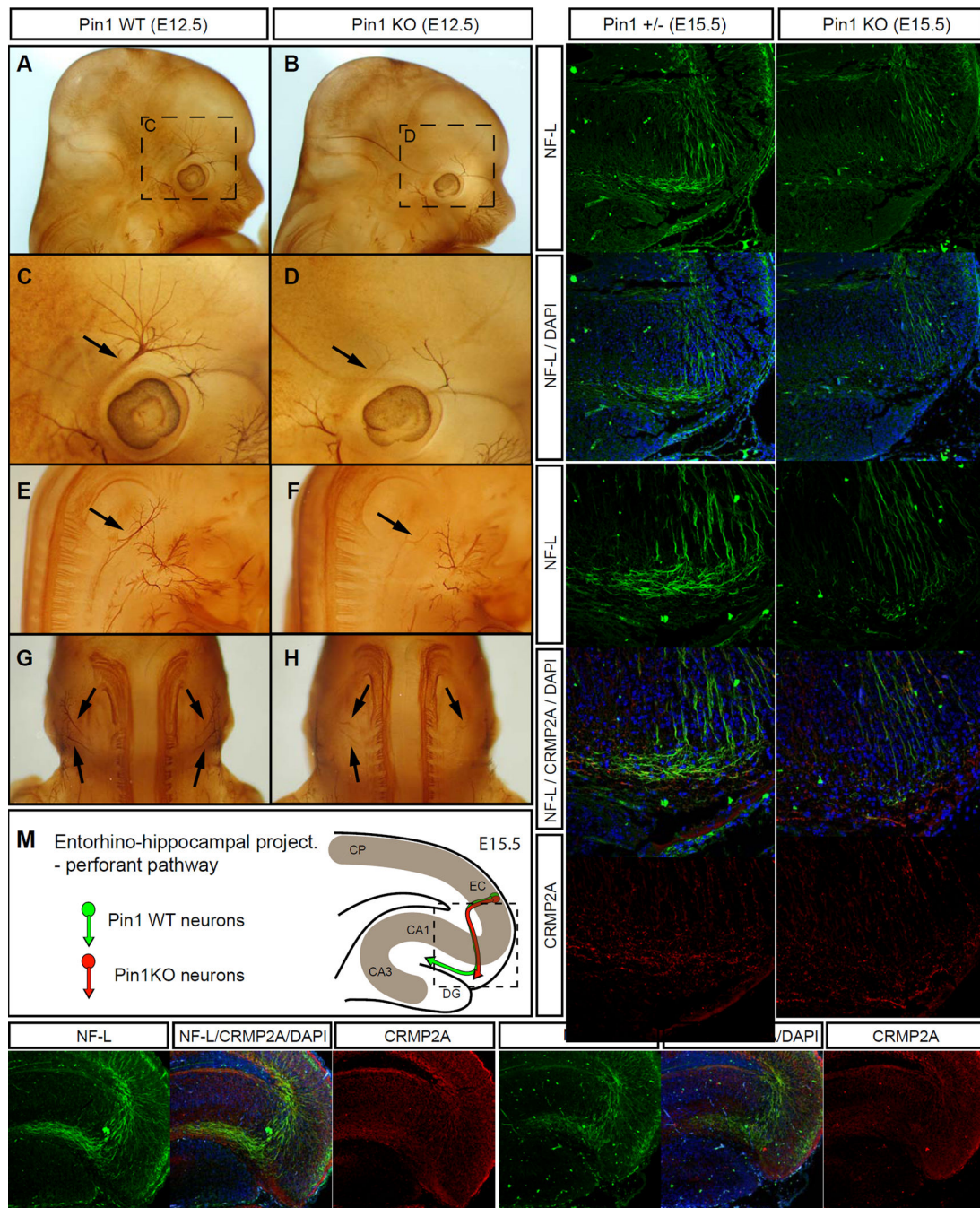
Figure 6. Pin1 KO leads to developmental axon growth defects in the peripheral and central nervous system

(A–H) Axons of the cranial and spinal nerves are less extensive and complex in Pin1 KO embryos. The cranial (A–D) and spinal (E–F) nerves were analyzed in E12.5 Pin1 WT (A, C, E, G) and KO (B, D, F, H) embryos by whole-mount immunohistochemistry for neurofilaments. In Pin1KO embryos stunted neurite processes are found in the ophthalmic branch of the trigeminal nerve (B, D, arrows) and in the lateral branches of the cervical spinal nerves (F, H, arrows). (I–M) Entorhino-hippocampal perforant projections are significantly shorter in Pin1 KO embryos at E15.5. Horizontal sections of E15.5 embryos

were stained for neurofilament light subunit (NF-L) (green) to trace growth of entorhinal perforant projections towards the stratum lacunosum-moleculare (s.l-m) of the hippocampus proper in Pin1+/− (I) and KO (J) mice. The dashed lines indicate borders of the developing dentate gyrus. (K, L) Pin1 KO shorter perforant projections are associated with reduced CRMP2A level (red) in growth cones, as pointed by arrows. (M) Schematic drawing of the entorhino-hippocampal perforant pathway at E15.5 in the presence or absence of Pin1 as shown in I-L. (CP - cortical plate, EC – entorhinal cortex, DG – dentate gyrus, CA1, CA3 – hippocampal regions). (N, O) Developmental defects are corrected later during development of Pin1 KO mice. Entorhinal perforant projections are detected in s.l-m of both Pin1 WT (N, arrow) and KO (O, arrow) newborn mice. Lower levels of CRMP2A are present in perforant projections in s. l-m in Pin1 KO mice (O) (Scale bars: I, J, N, O 100μm; K, L , 50 μm). See also Figure S5.
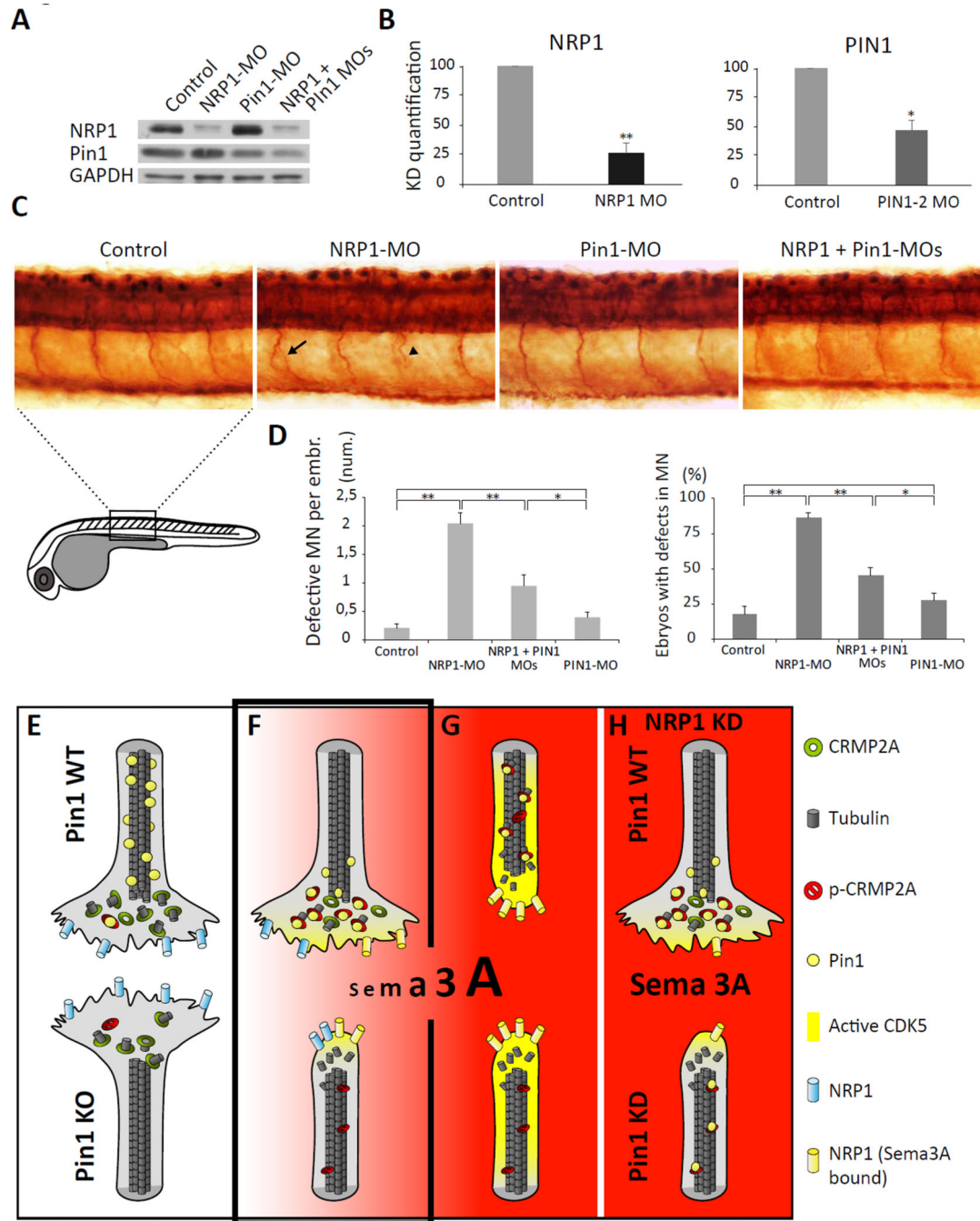
Figure 7. Pin1 regulates Sema3A signaling in vivo

(A, B) Efficiency of single and double morpholino KD of zPin1 and NRP1 in 24-h zebrafish embryos analysed by immunoblotting (A), quantification in (B). (C) Whole mount immunostaining of acetylated tubulin in 1-day-old zebrafish embryos demonstrates increased incidence of developmental motor neurons defects e.g. aberrant branching (arrow) or truncated growth (arrowhead) upon NRP1 KD, which is reduced upon co-injection of Pin1-MO. (D) Quantification of developmental defects in morpholino-injected zebrafish embryos. Control embryos and Pin1-MO injected do not significantly differ in percentage of

defective embryos (17% vs. 27% respectively) or average number of defects per embryo (0.22% vs. 0.4% respectively). NRP1 KD induces defective development in 85% of embryos, with the average of 2.05 defects per embryo. Co-injection of Pin1-MO significantly reduces number of defective embryos (44%) as well as the average number of defects per embryo (0.95). (E–H) A model of the Pin1 role in Sema3A-driven axonal growth/retraction.